PREDICTIVE POWER ESTIMATORS IN CDMA CLOSED LOOP POWER CONTROL

J. M. A. Tanskanen, A. Huang, and I. O. Hartimo

Lab. of Signal Processing and Computer Technology, Institute of Radio Communications
Helsinki University of Technology, P.O.Box 3000, FIN-02015 HUT, Finland

Abstract — In this paper, estimation of signal power is considered. Methods of designing optimized and partially-optimized power estimators, based on the Wiener model, for complex-valued signals are presented. Our application is predictive received power level estimation in closed loop transmitter power control of mobile CDMA communications systems. The proposed estimators have the benefits of guaranteed positive output, high computational efficiency as compared to quadratic filters, and providing for a predescribed prediction step, all the aspects being of great interest when applying the estimators in delay sensitive closed control loops. User capacity of a CDMA communications system is generally found to be greatly interference limited, and thus proper power control system functioning is of paramount interest. The partially-optimized power estimators are simulated along with Heinonen-Neuvo polynomial predictors in single- and multiuser CDMA uplink closed power control loop simulators.

I. INTRODUCTION

It has been recognized that power control is crucial to the performances of mobile radio communication systems, especially of the mobile CDMA systems [1][2]. In this paper, the objective of the power control is to maintain the powers received from individual users at an equal and constant level in order to maximize the user capacity of the communications system. The powers of the received noisy baseband signals are measured, filtered and compared with a preset power level threshold, so that power control can be realized by a closed control loop, and mutual interference between different users can be reduced. A lot of efforts have been made to improve power control efficiency [1][2][4][5]. Replacing power measurement with a predictive power estimator in the power control loop has been suggested [6][7] to combat background noise and interference corrupting the received power level estimates, and to compensate for control loop delays. In other words, the function of the predictive power estimator is threefold: to reduce additive noise and corrupting interference (i.e., filtering function), to calculate the received signal power level which is affected by channel fading and the distance between the mobile handset and the base station (i.e., measuring function), and to predict future values of the received signal power. Predictive power estimator reduces to power measurement if its filtering/prediction function is removed.

Power estimator is also called an energy estimator or energy detector [8][9], since power is actually instantaneous energy. Power estimator is doomed to be a nonlinear system because power is defined as the square of the signal magnitude. The available power estimators were developed for real-valued signals [1][2][3]. The standard energy detector consists of a linear time invariant (LTI) filter followed by a magnitude-square operation [1]. It has a simple structure and is thus computationally every efficient. However, the estimation bias at its output is not avoidable. A more general power estimator is called a quadratic filter (QF) or quadratic detector [1][2]. It can provide better trade-off between different desired features [2]. However, large processing delay and heavy computational requirements of quadratic filtering preclude its real-time use. Moreover, the resulting power estimate is not guaranteed to be positive.

In this paper, we propose an optimum power estimator (PE) for complex-valued signals, with application in closed power control loops of mobile communication systems. PE has a structure based on the Wiener model (WM) [1][2][8][9], and it is thus computationally very efficient. In this paper, PEs are designed to be one-step-ahead predictive. Also, their output is guaranteed to be positive as natural for power estimation applications. In Section II, the PE structure is presented, and two methods for optimum design are derived. Also, in Section II, the other simulated predictors are shortly reviewed, and the predictor parameter selection method used is described. The simulators are described, and simulation results given in Section III. Finally, Section IV summarizes the paper.

II. POWER ESTIMATOR IN BASEBAND

A. *Structure and Analysis*

For complex baseband signals, we construct a PE with two WMs and an adder, as shown in the dashed box in Fig. 1. The output of the system is estimated *power* of the input signal, rather than an estimate of the input signal itself. The filters in both WMs are of FIR type. They are usually chosen to be equal according to the assumptions on the input which will be addressed later. Their real impulse response $h(n)$ is designed due to the characteristics of the input. WM can be viewed as a special case of QF, or of the Wiener system used for nonlinear system recognition [1][2][8][9]. It has been called the standard energy detector for real-valued signals because its structure reflects the function of removing noise and then calculating signal power. Similarly, we call the PE in Fig. 1 standard PE for complex-valued signals. Its simple structure ensures computational efficiency.

Input signal consists of a signal component $x(n)=x_R(n)+jx_I(n)$ and noise/interference component $w(n)=w_R(n)+jw_I(n)$. The real, i.e., in-phase, part $x_R(n)$ and imaginary, i.e., quadrature, part $x_I(n)$ are assumed uncorrelated, and both are wide-sense stationary with known and usually *equal* statistics. The real part $w_R(n)$ and imaginary part $w_I(n)$ of noise are assumed to

be uncorrelated, and both are white Gaussian noise (WGN) processes with zero mean, equal variance $\sigma_w^2/2$ and kurtosis $3\sigma_w^4/4$ [10]. Hence, $w(n)$ is an additive WGN (AWGN) process with zero mean, variance σ_w^2 and kurtosis $2\sigma_w^4$ [7]. Input signal-to-noise ratio (SNR) γ is defined as the ratio of average powers of the input *signal* and *corrupting noise*

$$\gamma = E\{|x(n)|^2\}/E\{|w(n)|^2\} = R_x(0)/\sigma_w^2, \quad (1)$$

where $E\{\cdot\}$ denotes the expectation, $R_x(l)$ is the autocorrelation function whose value at the origin is the average power $R_x(0)$ of the signal.

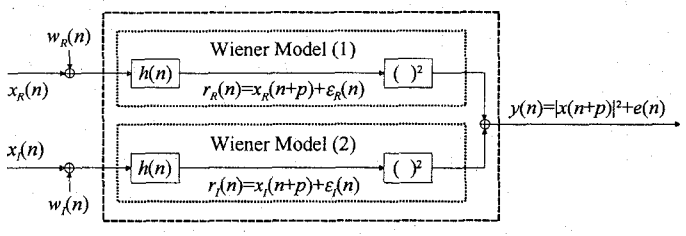

Fig. 1 The standard power estimator for baseband signals.

The output $y(n)=|x(n+p)|^2+e(n)$ is an estimate of the signal power $|x(n)|^2$ with a prediction step p. The value of p can be any integer depending on the underlying application, for instance, $p>0$ refers to p-step-ahead power prediction. The output $y(n)$ can also be expressed in terms of the filtered input $r(n)$ as

$$y(n) = r_R^2(n) + r_I^2(n) = |r(n)|^2 = r(n)r^*(n), \quad (2)$$

where $r(n) = r_R(n)+jr_I(n) = \mathbf{h}^T(\mathbf{x}+\mathbf{w})$ with the length-N filter impulse response vector $\mathbf{h} = [h(0) \ldots h(N\text{-}1)]^T$, the signal vector $\mathbf{x} = [x(n) \ldots x(n\text{-}N\text{+}1)]^T$, and the noise vector $\mathbf{w} = [w(n) \ldots w(n\text{-}N\text{+}1)]^T$. The superscripts "*" and "T" denote complex conjugate and transpose, respectively.

The real-valued power estimation error is defined as the difference between the actual and the desired outputs,

$$e(n) = y(n) - |x(n+p)|^2. \quad (3)$$

This error consists of the second-order terms $x^2(n)$ and $w^2(n)$, as well as the cross term of $x(n)$ and $w(n)$, due to the nonlinear operation. That is, this error is both signal-dependent and noise-dependent. The estimation bias is the mean value of $e(n)$,

$$Bias = E\{e(n)\} = E\{y(n)\} - R_x(0), \quad (4)$$

where the second equality holds according to the stationarity of $x(n)$. This bias is unavoidable because of the existence of the second-order terms in the expression of $e(n)$. The mean squared error (MSE) of the estimate $y(n)$ can be expressed as

$$E\{e^2(n)\} = E\{y^2(n)\} - 2E\{y(n)|x(n+p)|^2\} + E\{|x(n+p)|^4\}. \quad (5)$$

In the following, in order to minimize or reduce the MSE (5), we develop two methods to optimize the PE. The bias (4) is also reduced when the MSE is minimized or reduced.

B. *Global Optimization Method*

The global optimization is performed to design the FIR filters to minimize the MSEs $E\{e^2(n)\}$ at the output of the PEs. The output can be rewritten as $y(n) = \mathbf{h}^T(\mathbf{x}+\mathbf{w})(\mathbf{x}+\mathbf{w})^{*T}\mathbf{h} = \mathbf{h}^T\mathbf{S}\mathbf{h}$ since $r(n) = \mathbf{h}^T(\mathbf{x}+\mathbf{w}) = (\mathbf{x}+\mathbf{w})^T\mathbf{h}$ and $\mathbf{h}$ is real. Here $\mathbf{S} = \mathbf{S}^{*T} = (\mathbf{x}+\mathbf{w})(\mathbf{x}+\mathbf{w})^{*T}$ is a Hermitian matrix. Setting the partial derivative of (5), with respect to $\mathbf{h}$, to zero yields

$$E\{(\mathbf{S}+\mathbf{S}^*)\mathbf{h}_G\mathbf{h}_G^T\mathbf{S}\} = E\{|x(n+p)|^2 \cdot (\mathbf{S}+\mathbf{S}^*)\}, \quad (6)$$

where the subscript "G" denotes global optimization. Equation (6) cannot be further simplified due to the existence of the expectations. It provides an implicit expression for iteratively calculating the optimal filter impulse response $\mathbf{h}_G$ for a globally-optimized PE. However, the numerical calculations could be massive and possess some uncertainty in the obtained $\mathbf{h}_G$, and also convergence is not guaranteed.

C. *Partial Optimization Method*

Let the filtered input signal in Fig. 1 be expressed as $r(n)=x(n+p)+\varepsilon(n)$, where $\varepsilon(n)=\varepsilon_R(n)+j\varepsilon_I(n)$ is the estimation error at the output of the FIR filters. The goal now is to minimize the MSE $E\{|\varepsilon(n)|^2\}=E\{\varepsilon_R^2(n)\}+E\{\varepsilon_I^2(n)\}$ so that an *optimal estimate of the delayed signal* is achieved at the output of the filters, and the MSE $E\{e^2(n)\}$ at the PE output is in turn reduced. In other words, the overall PE is partially optimized.

The optimal filters minimizing $E\{\varepsilon_R^2(n)\}$ and $E\{\varepsilon_I^2(n)\}$ are simply the Wiener filters. Their impulse responses are equal according to the assumptions on the input signal and noise, and can be calculated from the Wiener-Hopf equation [11]

$$\mathbf{h}_{opt} = \mathbf{R}_R^{-1}\mathbf{r}_R, \quad (7)$$

where $\mathbf{R}_R = E\{(\mathbf{x}_R+\mathbf{w}_R)(\mathbf{x}_R+\mathbf{w}_R)^T\}$ is an $N\times N$ auto-correlation matrix, $\mathbf{r}_R = E\{x_R(n+p)[\mathbf{x}_R+\mathbf{w}_R]\}$ is a cross-correlation vector, and $\mathbf{x}_R$ and $\mathbf{w}_R$ are the real parts of $\mathbf{x}$ and $\mathbf{w}$, respectively. Since noise $w(n)$ is WGN and independent of $x(n)$, further derivation yields

$$\mathbf{h}_{opt} = \left(\mathbf{R}_{xR} + \sigma_w^2\mathbf{I}/2\right)^{-1}\mathbf{r}_{xR}, \quad (8)$$

where $\mathbf{R}_{xR} = E\{\mathbf{x}_R\mathbf{x}_R^T\}$ and $\mathbf{r}_{xR} = E\{x_R(n+p)\mathbf{x}_R\}$. The partial optimization approach is of practical interest due to its simple and closed-form solution.

It can be seen from (8) that a prototype signal $x(n)$ and noise variance are needed to calculate the optimal impulse response, and also the filter length N has to be specified. The following study on parameter selection provides a method of choosing filter length N and prototype signal length L.

One-step-ahead predictive Wiener filters of lengths N=1~50 are designed for each mobile speed 5, 10, ..., 45 km/h and prototype signal length L=300, 600, ..., 15000 samples. In-phase and quadrature components of Rayleigh fading signals, whose components are corrupted with AWGN with variances 0, 0.05, 0.1, 0.2, 0.3, ..., 0.9, 1, and 5 are employed as prototype signals. The resulting Wiener filters are tested by estimating one-step-delayed test signals with the same statistics as the prototype signals. The MSEs $E\{\varepsilon_R^2(n)\}$ and $E\{\varepsilon_I^2(n)\}$ at the filter outputs are calculated for each case, and an error surfaces versus L and N are formed. The values of N and L corresponding to minimum MSEs are then obtained. For simplicity, we use "optimal predictor" in the following to indicate the predictive Wiener filter designed based on the N and L values determined.

Magnitude responses of three optimal predictors are shown in Fig. 2. It can be seen that for the low-noise cases, the pre-

dictor band-width generally grows with the received fading signal band-width which is proportional to the mobile speed. At high noise cases, the predictor design favors noise reduction, even with the cost of payload signal degradation.

Figure 3 depicts an MSE surface for the low-noise, 10 km/h case. The optimum predictor is found with predictor length N=50, designed using a prototype signal of L=13200 in-phase component samples. It is seen that the MSE error surface has a fairly large flat area which is also equally evident in all the other error surfaces in our studies. This flat area is due to the fact that the optimization of the predictor coefficients is done according to the predefined N, and the fact that a prototype signal segment of sufficient length reflects the statistics of the signal with high probability. In other words, the choice of predictor length N is quite free and the selection of L is also flexible within a fairly large region. All the error surfaces greatly resemble that seen in Fig. 3. The MSE surfaces for the higher mobile speeds exhibit "wavy" behavior below certain prototype signal lengths, and optimum predictors with lengths within that region would be dangerously specific to the statistics of the prototype signal, although from the signal statistics point of view it may seem illogical to use longer prototype signals for higher mobile speeds. Since the resulting region of N is more or less dependent on the choice of the prototype signal, not all predictors designed are always optimal for the actual overall

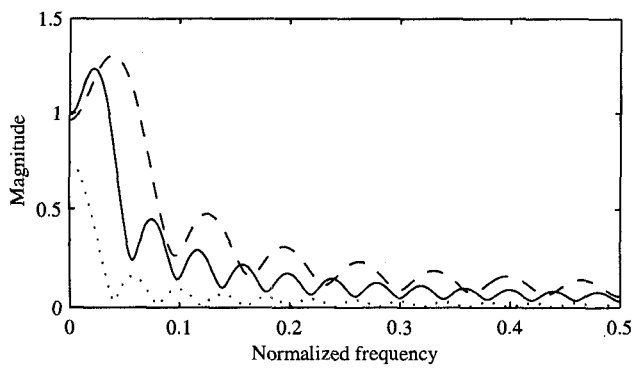

Fig. 2 Frequency responses of the optimal predictors designed for 10 km/h (solid) and 30 km/h (dashed) with component noise variance 0.05, and for 30 km/h and noise variance of 5 in components (dotted). Note that the frequency scale is up to half the Nyquist rate.

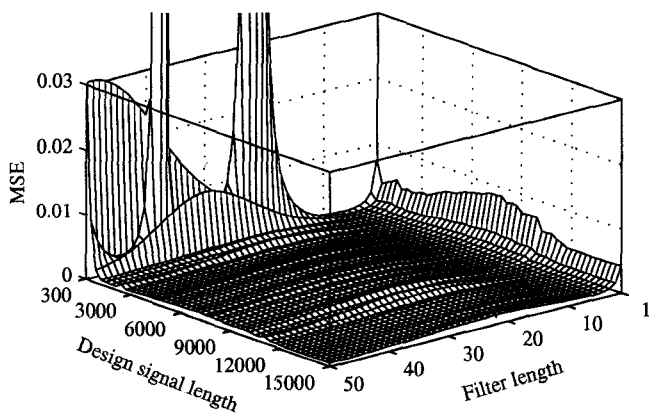

Fig. 3 The MSEs for the predictors designed for the mobile speed of 10 km/h and component noise variance 0.05. The optimal predictor is found to be of length N=50 designed using L=13200 in-phase component prototype signal samples.

signal statistics. It is to be stressed that the method of forming the MSE surface and searching the relevant N and L for optimal predictor design is actually not in any way related to the power control problem. Thus the described method serves only as a consistent and "scientific" way for selecting the predictor design parameters, instead of yielding the values of N and L optimal for the actual application. For the power control function it is beneficial to apply fairly short predictors within the flat nearly-optimal region. Reasonable guidelines are N=5~25 and L=3000~6000 for mobile speeds <20 km/h, and N=10~25 and L=6000~9000 for speeds >20 km/h.

In the following, we use optimum predictors designed with the parameters found from the error surfaces. It should be pointed out that some shorter ad hoc designed optimum predictors may actually yield as good results. Thus, also predictors with ad hoc design parameters, length N=15, designed with L=3000 samples, within the guidelines above, are also used in the simulations.

D. *Heinonen-Neuvo Polynomial Predictors*

Heinonen-Neuvo (H-N) polynomial predictors [13] are used in the simulations since Rayleigh fading signals can well be piecewisely approximated by polynomials. H-N predictors are optimized to minimize filter output noise power when the input is a noisy polynomial signal of a known degree. They are low-pass filters with, in this paper, group delays exactly minus one in narrow low frequency bands. Their coefficients have closed from solutions for each filter length and low polynomial input signal degree. Since the design of the H-N predictors does not employ prototype signals, the relevant values of the predictor length N and polynomial degree K are searched within the region N=5~50, K=1~3, by employing the same minimum MSE criterion as with the optimum estimators.

III. POWER CONTROL SIMULATIONS

To assess the applicability of the PEs to the closed loop power control in CDMA communication systems, a single-user simulator, multiuser simulators with 5 and 10 users, and a simulator with AWGN interuser interference model, are constructed in COSSAP software environment. The communications system parameters are selected as carrier frequency 1.8 GHz, chip rate 1.2192 MHz, bit rate 9600 Hz, control period 0.625 seconds, and single bit power control command with ±1 dB mobile transmitter power level change step. These parameters are derived from those for the Qualcomm CDMA system [12] except that the control rate is doubled, and 127 chips per bit is used instead of 128 chips per bit, which, with the bit rate, yields the mentioned chip rate. Resulting CDMA codes are not orthogonal; code autocorrelations yield 127, while the code cross correlations are equal to -1, introducing interuser interference. To evaluate system performance, bit error rates (BERs) are counted by comparing 100,000 bits of the received signal and the transmitted signal. Each user has a Rayleigh fading channel corresponding to his mobile speed, and the total control loop delay is set to 2 chip durations for all the users.

Four types of power controllers are tested: Controller 1 using partially-optimized one-step-ahead predictive PEs, Con-

troller 2 using PEs with one-step-ahead predictive H-N predictors, and the as the reference, Controller 3 using non-filtering power measurement. The partially-optimized PE with the ad hoc design parameters is employed in Controller 1'. The objective of the power control is to minimize the variance of the power level received from each individual user, i.e., variance of the user's radio channel output power, which is now our control variable.

A. *Singleuser System*

A singleuser simulator consists of a mobile transmitter, radio channel, base station receiver and power controller models. The radio channel is a Rayleigh fading channel [4], with the mobile speed set to 10 km/h or 30 km/h. AWGN is added independently to the in-phase and quadrature components. In Fig. 4, the component SNR axis labels correspond to the added component AWGN variances 0, 0.1, ..., 0.9, respectively.

In the singleuser simulator, the input to the power controller is the despread total received signal which is only decimated so that the controller input rate is the same as the bit rate. As all the received noise left after despreading is also fed to the controller, the predictors' noise reduction capabilities are more pronounced in the single user case than in the multiuser case.

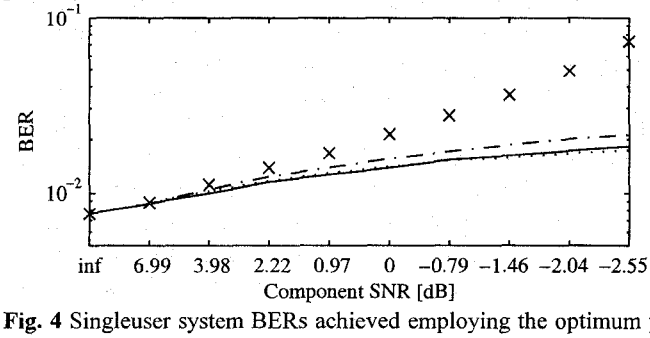

Fig. 4 Singleuser system BERs achieved employing the optimum predictors (solid), an ad hoc optimum predictor with N=15 (dotted), and H-N predictors (dash-dot) in the controllers, along with the BERs using the non-filtering reference controller (crosses) at the mobile speed of 30 km/h.

In Fig. 4, BERs from the single user simulations at 30 km/h are shown. It is clearly seen that as the noise level gets higher, the system with the non-filtering reference controller fails. This is due to the fact that as the received noise power increases, the power controller commands for lower transmitter power level. The systems with low-pass predictors are still functional under high noise conditions, with the optimum predictor providing for a little better achieved BERs. At 10 km/h, the conclusion on the necessity of the filtering remains equally clear, with all the corresponding BERs somewhat lower than those shown in Fig. 4. The partially-optimized PE is seen to yield slightly better performance than the H-N predictor. Also, there is little difference whether the design parameters of the partially-optimized PEs are optimized or selected ad hoc.

B. *Multiuser System*

In the multiuser simulators, input to the controller is the despread received signal which is integrated over the bit duration in order to produce an estimate of the bit energy received from a given user. Integration instead of decimation is the difference between the multiuser and the singleuser simulators. Integration naturally has the effect of removing some noise and interference from the controller input signal, and thus the predictors' actual predictive properties are more pronounced.

In the multiuser simulator, one user is observed. The speed of the observed mobile user is set to 10 km/h or 30 km/h, while the other interfering users' speeds v_i, i=1, ..., 9, are set to v_i=i·5 km/h, in the 10-user simulations, and to v_i=i·10 km/h, i=1, ..., 4, in the 5-user simulations. A user in a multiuser simulator is illustrated in Fig. 5. Receiver noise is simulated by adding AWGN with component variance 0.05. For other than mentioned simulator details, please refer to [14].

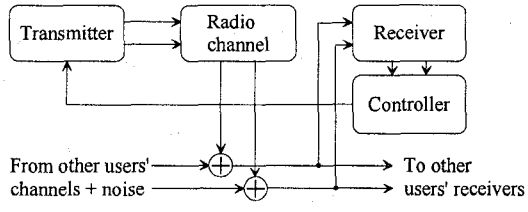

Fig. 5 Block diagram of a user in the multiuser communications system simulators.

The main multiuser simulation results are given in Tables 1, 2 and 3. The results also reflect relations between the simulated actual multiuser interference models and the commonly used AWGN multiuser interference model. From all the Tables 1, 2 and 3, it is seen that the multiuser and AWGN multiuser simulations yield somewhat different results. Conclusions on the effects of the predictors are dependent on the interference model used, which is mainly evident in Tables 2 and 3 describing transmitter power consumption savings and power control function performance improvements, respectively.

In Table 1, achieved BERs are listed. It is to be noted that these are 'raw' BERs, i.e., e.g. no error corrective coding is used. Thus, all other differences between BERs from the three predictive systems and the reference system are negligible in the sense of actual data transmission, except for the case where interference is modeled by a very high AWGN level under high mobile speed. In this case, the systems employing the optimum predictors are able to deliver 20~30 % less bit errors than the other two systems. From the corresponding results in Tables 2 and 3, it is seen that the cost of these BER improvements is increased power consumption and greater variance of the radio channel output power level, i.e., degradation of the control variable quality. The optimum PEs with the ad hoc design parameters, Controller 1', are seen to function as well as the ones with optimized design parameters. Generally, the previous ones deposit more transmitter power, which results in better BERs in the high level AWGN interference model cases.

In Table 2, transmitter power consumption savings from applying predictive filtering are listed. The results reflect the fact that H-N predictors are in most cases capable of slightly adjusting the control timing, resulting in a slightly decreased transmitter power consumptions while maintaining or even slightly decreasing the corresponding BERs. The improvements are more pronounced if the interference can be modeled by the AWGN. The effect of the optimum predictors is seen to be mostly that of depositing more transmitter power.

Table 3 presents the effects of the predictive power estimation to the control variable. If the system is modelable by the AWGN interference model, both H-N and optimum predictors can provide for substantial improvements in the power control operation in most of the cases. 50 % reduction in the variance of the received power level is expected to directly contribute to the communications system user capacity though this has not been explicitly tested yet. Controller 1' provides for slight power control function improvements also in all the actual multiuser simulation cases.

IV. SUMMARY

The Wiener model based computationally efficient power estimators for complex signals have been proposed. The output of the PE is guaranteed to be positive as naturally desirable for all applications requiring power estimation. Also, the PE can be designed to be predictive for delay sensitive control applications. For our application, predictive Rayleigh fading signal power estimation in closed power control loops, short filters with $5<N<21$ are found adequate. Simulation results are shown and compared with results from the corresponding non-filtering reference systems. The results demonstrate clear need for filtering within closed power control loops, while fine tuning the control system is found possible by applying proper predictive PEs. In practice, an adaptive algorithm can be used to adjust the partially-optimized PE to suit for actual channel variation and SNR [7].

ACKNOWLEDGMENTS

This project has been financed by the Technology Development Centre of Finland (TEKES), Nokia Corporation, Telecom Finland, and Helsinki Telephone Company, Finland. The work of J. M. A. Tanskanen has also been supported by the Päijät-Häme Fund under the Auspices of the Finnish Cultural Foundation, by Foundation of Technology, Finland, and by Jenny and Antti Wihuri Foundation, Helsinki, Finland.

REFERENCES

[1] G. Sicuranza, "Quadratic filters for signal processing," Proc. of the IEEE, vol. 80, no. 8, pp. 1263-1285, Aug. 1992.

[2] J. Fang and L. E. Atlas, "Quadratic detectors for energy estimation," IEEE Trans. Signal Processing, vol. 43, no. 11, pp. 2582-2594, Nov. 1995.

[3] J. F. Kaiser, "On Teager's energy algorithm and its generalization to continuous signals," Proc. IEEE Digital Signal processing Workshop, Mohonk (New Paltz), New York, Sept. 1990.

[4] K. Gilhousen, I. Jacobs, R. Padovani, A. J. Viterbi, L. A. Weaver, Jr., and C. E. Wheatley III, "On the capacity of a cellular CDMA system," IEEE Trans. Vehicular Technology, vol. 40, pp. 303-312, May 1991.

[5] O. K. Tonguz and M. M. Wang, "Cellular CDMA networks impaired by Rayleigh fading: system performance with power control," IEEE Trans. Vehicular Technology, vol. 43, pp. 515-527, Aug. 1994.

[6] J. Tanskanen, A. Huang, T. I. Laakso, and S. J. Ovaska, "Prediction of received signal power in CDMA cellular systems," in Proc. 45th IEEE Vehicular Technology Conference, Chicago, IL, July 1995, pp. 922-926.

[7] A. Huang, J. M. A. Tanskanen, and I. O. Hartimo, "Design of optimum power estimator based on Wiener model applied to mobile transmitter power control," in Proc. 1998 IEEE Int. Symposium on Circuits and Systems, Monterey, CA, USA, May 1998, in press.

[8] I. Pitas and A. N. Venetsanopoulos, Nonlinear Digital Filters. London, UK: Kluwer, 1990.

[9] T. Wigren, "Recursive prediction error identification using the nonlinear Wiener model," Automatica, vol. 29, pp. 1011-1025, 1993.

[10] C. L. Nikias, Higher-Order Spectral Analysis. Englewood Cliffs, NJ: Prentice-Hall, 1993.

[11] C. W. Therrien, Discrete Random Signals and Statistical Signal Processing. Englewood Cliffs, NJ: Prentice-Hall, 1992.

[12] QUALCOMM Incorporation, An Overview of the Application of Code Division Multiple Access (CDMA) to Digital Cellular Systems and Personal Cellular Networks (Document no. EX60-10010), 1992.

[13] P. Heinonen and Y. Neuvo, "FIR-median hybrid filters with predictive FIR substructures," IEEE Trans. ASSP, vol. 36, no. 6, pp. 892-899, June 1988.

[14] J. Tanskanen, J. Mattila, M. Hall, T. Korhonen, and S. J. Ovaska, "Predictive closed loop power control for mobile CDMA systems," in Proc. 47th IEEE Vehicular Technology Conference, Phoenix, AZ, USA, May 1997, pp. 934-938.

Table 1. BERs from the simulations of 100000 bits with the total control loop delay of 2 chip durations, and observed user's speeds 10 km/h and 30 km/h, for 5 and 10 users, and for AWGN interference models with component noise variances of 1 and 5.

Controller	5 users 10 km/h	5 users 30 km/h	10 users 10 km/h	10 users 30 km/h	AWGN interf. 10 km/h, var = 1	AWGN interf. 10 km/h, var = 5	AWGN interf. 30 km/h, var = 1	AWGN interf. 30 km/h, var = 5
1) optim. pred.	$5.3\cdot10^{-3}$	$10.0\cdot10^{-3}$	$6.6\cdot10^{-3}$	$11.8\cdot10^{-3}$	$10.8\cdot10^{-3}$	$22.7\cdot10^{-3}$	$17.1\cdot10^{-3}$	$31.2\cdot10^{-3}$
1') optim. ad hoc pred., N=15	$5.2\cdot10^{-3}$	$10.3\cdot10^{-3}$	$6.6\cdot10^{-3}$	$11.8\cdot10^{-3}$	$9.9\cdot10^{-3}$	$20.2\cdot10^{-3}$	$16.3\cdot10^{-3}$	$26.6\cdot10^{-3}$
2) H-N pred.	$5.2\cdot10^{-3}$	$9.8\cdot10^{-3}$	$6.6\cdot10^{-3}$	$11.6\cdot10^{-3}$	$9.8\cdot10^{-3}$	$22.1\cdot10^{-3}$	$19.0\cdot10^{-3}$	$42.8\cdot10^{-3}$
3) reference	$5.1\cdot10^{-3}$	$10.2\cdot10^{-3}$	$6.6\cdot10^{-3}$	$11.8\cdot10^{-3}$	$11.3\cdot10^{-3}$	$24.4\cdot10^{-3}$	$18.8\cdot10^{-3}$	$40.4\cdot10^{-3}$

Table 2. Power savings achieved employing the prediction from the same simulations as in Table 2.

Controller	5 users 10 km/h	5 users 30 km/h	10 users 10 km/h	10 users 30 km/h	AWGN interf. 10 km/h, var = 1	AWGN interf. 10 km/h, var = 5	AWGN interf. 30 km/h, var = 1	AWGN interf. 30 km/h, var = 5
1) optim. pred.	-0.2 %	-0.5 %	0.4 %	-0.5%	0.6 %	-16.2 %	-6.6 %	-51.0 %
1') optim. ad hoc pred., N=15	-0.6%	-2.1%	-0.6%	-2.2%	-3.0%	-29.5%	-14.1%	-56.8%
2) H-N pred.	0.5 %	0.4 %	-0.3 %	0.4	5.9 %	4.4 %	8.0 %	6.0 %

Table 3. Channel output variance reductions achieved by applying the prediction from the same simulations as in Table 2.

Controller	5 users 10 km/h	5 users 30 km/h	10 users 10 km/h	10 users 30 km/h	AWGN interf. 10 km/h, var = 1	AWGN interf. 10 km/h, var = 5	AWGN interf. 30 km/h, var = 1	AWGN interf. 30 km/h, var = 5
1) optim. pred.	2.7 %	-1.0 %	-1.4 %	-3.1 %	59.2 %	41.7 %	50.3 %	-111.7 %
1') optim. ad hoc pred., N=15	1.3%	2.7%	1.4%	1.1%	51.6%	26.4%	39.8%	-75.2%
2) H-N pred.	-0.9 %	1.4 %	-0.8 %	0.3 %	58.0 %	54.9 %	68.0 %	62.1 %